Journal of the Korean Ceramic Society
Vol. 42, No. 11, pp. 703~717, 2005.

Infiltration Processing of Ceramic-Metal Composites: The Role of Wettability, Reaction, and Capillary Flow

Rajiv Asthana, Mrityunjay Singh,*† and Natalia Sobczak**

Engineering and Technology Department, University of Wisconsin-Stout, Menomonie,WI 54751, U.S.A.
**QSS Group, Inc., NASA Glenn Research Center, Cleveland, OH 44135, U.S.A.*
***Department of Physical Chemistry of Metals and Alloys, Foundry Research Institute, Krakow, POLAND*
(Received October 11, 2005; Accepted November 1, 2005)

ABSTRACT

The infiltration of ceramics by liquid metals to fabricate ceramic-metal composites is discussed. In particular, the complexity of infiltrating ceramics by liquid metals at high temperatures due to interfacial reactions, metal oxidation, pore modulation and closure, and transient capillary forces has been highlighted. The role of these factors is discussed in the context of reactive infiltration with examples from ceramic/metal composites of practical interest. In addition to flow through porous ceramics, reactive penetration of dense ceramics via chemical dissolution and reaction is also discussed.

Key words*: *Infiltration, Ceramic-Metal Composite, Wettability, Penetration, Capillary flow, Joining

1. Introduction

Infiltration of ceramics by liquid metals is a widely used technique to synthesize ceramic-metal composites. Infiltration is also encountered in coatings, sealing, brazing, sintering, and numerous other processes. The flow of metals through porous ceramics is either spontaneous, driven by self-sustaining capillary forces, or it may require external pressure (delivered by vacuum suction, hydraulic rams, inert gas, centrifugal force, or electromagnetic field) when the poor wettability of the solid ceramic inhibits spontaneous wetting. The complexity of infiltrating ceramics by liquid metals at elevated temperatures is compounded by surface roughness, chemical inhomogeneity, variable cross-section and pore morphology, tortuosity, and partial solidification (if the ceramic is sub-cooled with respect to the invading metal), and reaction layer formation, both of which may lead pore closure and flow cessation. The flow may be multi-directional, accompanied by exothermic chemical reactions and dissolution processes that release chemical species in the flowing liquid, and modulate the thermal and diffusional fields. Reactions can also cause time-dependent changes in the solid/liquid (S/L) interface, and in the capillary forces driving the flow. Fluid shear may redistribute the solutes and rearrange loosely-packed particulate ceramics.

Infiltration pervades numerous technical fields,[1-10] and boasts of rich and eclectic technical literature that integrates theories of surface physics, hydrology, thermal and fluid sciences, materials science, chemical engineering, and high-temperature chemistry, thus permitting knowledge crossover and exchange between disciplines. This presents both a challenge and an opportunity to study the various facets of infiltration from different points of view. In this review, we discuss the infiltration of ceramics by liquid metals, focusing on some aspects of wetting, reactivity, and metal flow primarily in porous ceramics. In addition to capillary-driven flow through porous ceramics, reactive penetration of dense ceramics via chemical dissolution and reaction is also discussed.

†Corresponding author : Mrityunjay Singh
E-mail : msingh@grc.nasa.gov
Tel : +1-216-433-8883 Fax : +1-216-433-5544

2. Infiltration of Porous Ceramics

Fig. 1 shows examples of ceramic-metal composites synthesized by liquid metal infiltration of technical ceramics with micrometer-size pores, such as SiC platelets and sapphire fibers. The metal crystallizes within the pores to form the usual solidification microstructure but with some modifications caused due to the constrained solidification within fine pores (e.g., reduced amount of eutectic and secondary phases, reduced segregation in fine pores, etc). Reactive solutes in the liquid matrix may attack the ceramic phase causing its dissolution. Poorly wetting ceramics require external pressure to initiate the flow. When performs made of ceramic fibers are used, are must be taken to minimize fiber damage, preform distortion, and uneven fiber distribution under external pressure. Fiber-to-fiber contact at large fiber fractions may lead to metal-starved regions that may become crack initiation sites upon solidification. Processing conditions must be carefully designed to avoid these problems.

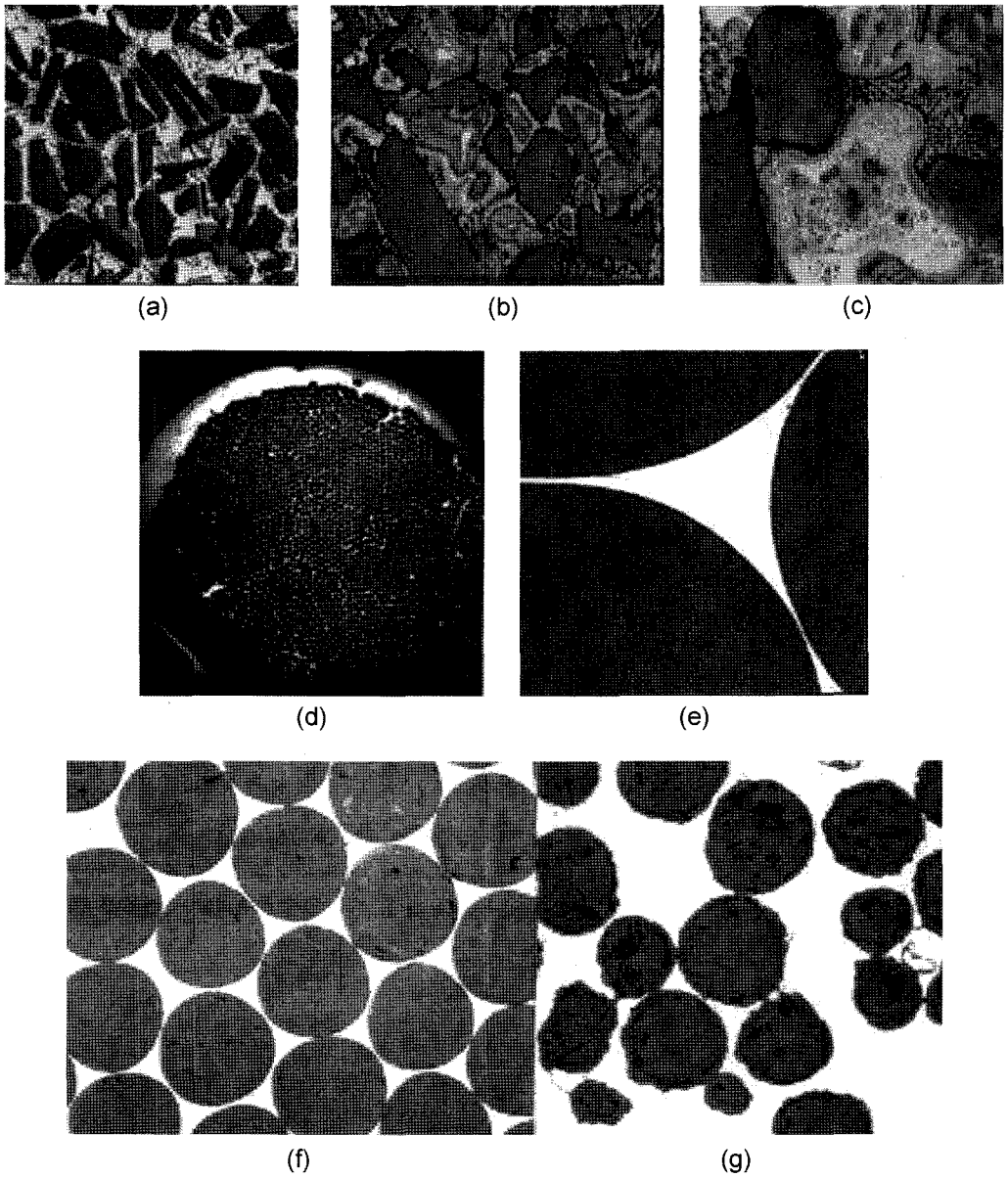

Fig. 1. Melt infiltrated SiC/2014 Al composite (a)-(c), and sapphire/Ni-superalloy composite (d)-(g). (b)-(c) show cored dendrites, (d)-(g) show fiber distribution, interfiber channels, and chemical attack of sapphire by the superalloy.

2.1. Threshold Pressure

The onset of flow in non-wetting ceramics occurs when the fluid pressure at the liquid front exceeds a critical or threshold pressure, P_{th}.[1,2,11-23] Fig. 2(a) displays the measured P_{th} as a function of particle diameter, D, in some ceramic/metal systems. The diameter, D, is related to the effective pore size; in randomly packed beds, the effective pore radius, R, is taken to be the hydraulic mean radius. The data of Fig. 2(a) show that P_{th} varies inversely with D, which is consistent with the Young-Laplace equation for capillary pressure, P_c ($P_c = -2\sigma_{LV}\cos\theta/R$, where σ_{LV} is the surface tension of the liquid, and θ is the contact angle, defined from the Young-Dupre equation, $\sigma_{SV} = \sigma_{LS} + \sigma_{LV}\cos\theta$, and σ's are the interfacial energies of solid (S), liquid (L), and vapor (V), respectively). Thus, P_{th} may be regarded as a practical measure of P_c in high-temperature ceramic/metal systems. From the Young-Laplace equation it is noted that an acute θ ($\theta < 90°$) yields a negative value of P_c, indicating spontaneous wetting and self-infiltration ('wicking'), which is utilized for pressureless infiltration to fabricate the composites.[24-28] The threshold pressure also depends upon particle shape, and is found to be greater for ceramic platelets of high aspect ratio, which tend to form narrow wedge-shaped capillaries due to preferred orientation and stratification, than nodular particles.[1,13,22]

During flow through ceramics, liquid metal may encounter chemical inhomogeneity and roughness which impair the wettability and reduce the capillary forces. Contact

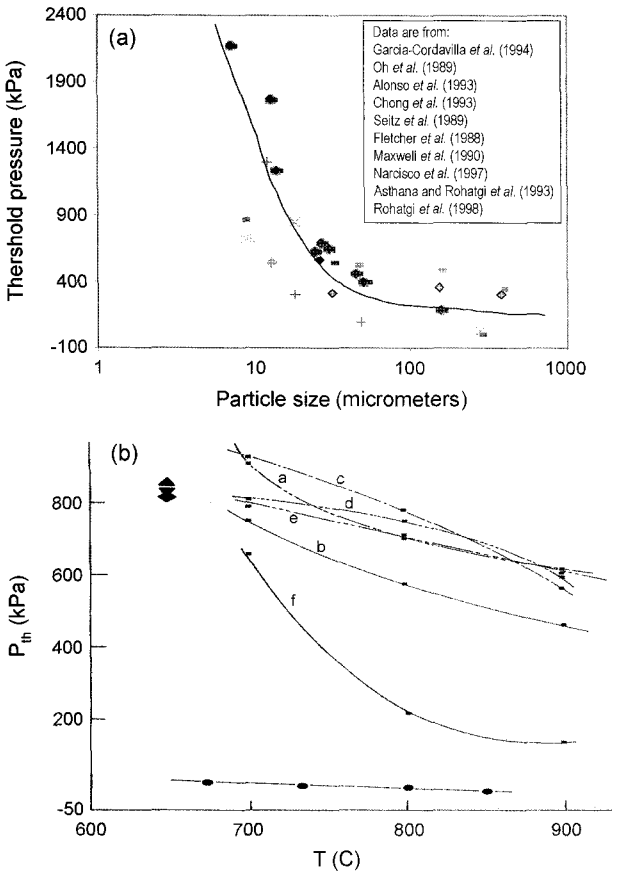

Fig. 2. (a) Literature data on threshold pressure of Al in SiC, B_4C, TiC and Al_2O_3, and (b) the effect of temperature on the P_{th} of Al and Zn alloys in SiC and B_4C.

angles given by the Young-Dupre equation apply to ideal surfaces. Real surfaces are chemically and structurally inhomogeneous, and consist of grooves, ridges, grain boundaries, dislocations, adsorbed films, and oxidized, corroded or coated areas, as well as crystal planes of different atomic density. The liquid front on a real surface does not retrace its path during forward and receding motions, and the contact angles are different during advance and recession. This gives rise to contact angle hysteresis, which increases with increasing roughness. The scale of roughness, metal velocity, and temperature determine the effect of roughness on flow. At large velocities in forced flow, liquid front 'slips' over asperities without penetrating the wedges whereas at low velocities, the front advances by 'stick-slip' motion. At very high temperatures, roughness effects on wetting may be masked by the thermal energy.

Both the liquid surface tension, σ_{lv}, and contact angle, θ (and, therefore, P_c) depend upon temperature, atmosphere, and liquid composition.[12-14,29] Experiments show that P_{th} decreases with increasing temperature (Fig. 2(b)), which is a consequence of the improved wettability at elevated temperatures. However, high temperatures are beneficial only under a 'clean' atmosphere in which the wettability-inhibiting surface oxides are unstable. In fact, the experimentally measured P_{th} is frequently found to be nearly the same for different types of ceramics such as SiC, TiC, and Al_2O_3 when they are infiltrated at a constant temperature by molten Al in air.[1] This is contrary to the sessile-drop measurements of wettability at similar temperatures which show that these particulates form different contact angles with Al under controlled test environment.[30,31] Inert and/or reducing atmospheres ($Ar + H_2$) and metal-coated ceramics[32] yield low values of P_{th}. Thus surface oxides obstruct attainment of wettability even at high temperatures under oxidizing atmospheres, and to realize the benefits of improved wettability at high temperatures, it is imperative to utilize an oxygen-deficient atmosphere. Most in-situ composite growth techniques utilize controlled atmosphere and wetting-promoters (e.g., Mg) to reduce the oxidation and create large negative capillary pressures to cause self-infiltration ('wicking'). In most cases, a critical level of the wetting promoter such as Mg is needed. Self-infiltration has been profitably used to fabricate a variety of ceramic- and metal-matrix composites. The composite forms by growth of multi-phase layers at the reaction front, which consist of MgO and $MgAl_2O_4$. Microchannels in these layers allow 'wicking' of the melt to the free surface and continuation of composite growth. The growth rate is limited by the supply of metal at the reaction front, and the transport of oxygen through grain boundaries, microcracks and pores in surface layers. If all the metal is used up, porous microstructures form. Self-infiltration is, however, slow, and can take several hours to form the composite.

The experimental dependence of P_{th} on D (Fig. 2(a)) suggests that extremely large pressures are needed for infiltration of very fine ceramics. Recent studies[33] have shown that pressures on the order of ~2 – 8 GPa are needed to infiltrate Al_2O_3, SiC and diamond nanoparticles by Mg, Sn, Zn, Al, Ag, Cu, and Ti. Fine pores may approach the atomic lattice size in crystals, making it prohibitively difficult to infiltrate such pores even though there may be technological benefits in doing this. Consider the intriguing possibility of infiltrating ropes made from carbon or boron nitride nanotubes with liquid metals to produce ultra high-strength ceramic/metal composites. The spacing between the individual strands in such ropes is in the sub-nanometer range, e.g., ~0.34 nm in ropes made from multi-walled BN nanotubes,[34] which is on the order of the (0001) lattice spacing in hexagonal BN. Infiltration of such atomic size pores using conventional techniques in the absence of surface modification to improve the wettability may be forbidden due to the prohibitively large pressures needed to initiate the flow.

2.2. Effect of Oxide

Oxygen strongly influences the infiltration and spreading behavior of metals on ceramics. Metal/oxide couples with very low quantities of dissolved O in the liquid metal (from the dissolution of the substrate) exhibit large q because of purely physical (dispersion) forces[30] at the interface. For non-reactive couples with more dissolved O from the sub-

strate, the Me-O clusters are adsorbed at the interface, and yield relatively low θ values. The lowest θ values are achieved in reactive Me/oxide couples that form reaction products with metal-like character. However, undissolved residual oxygen in the infiltration atmosphere will inhibit the spreading by forming tenacious oxide skin on the liquid front, which will resist metal flow and hinder ceramic/metal contact. This will adversely influence not only the θ value, but also the metallurgical structure and adhesion at the interface.

The negative effects of oxide films on ceramic/metal wettability are clearly revealed in sessile-drop tests that utilize a Capillary Purification (CP) technique[35] to erode the surface oxides by extruding tiny droplets of liquid metals through a graphite syringe just prior to contact with the substrate under high vacuum (or under inert atmosphere). Fig. 3(a) compares the contact angle, θ, of Al/Al_2O_3 sessile-drop couples made using two different wettability test procedures: Contact Heating (CH) in which the metal and substrate are jointly heated to the test temperature, and the capillary purification technique (CP). The data of Fig. 3(a) reveal the benefit of mechanical removal of surface oxides on the contact angle; a low θ is obtained with the CP procedure even at relatively low temperatures. Such low θ values are attained in CH only at significantly higher temperatures where oxide dissociation permits physical contact. Fig. 3(b) shows the measurements of interfacial shear strength, τ, in CH and CP Al/Al_2O_3 couples which also confirms the beneficial effects of oxide removal by CP. The shear strength measurements were made using an improved droplet push-off technique[35-40] in which the solidified sessile-droplet bonded to the ceramic substrate are bisected using a precision cutter along their diameter, and shear stress is applied to the flat (cut) face of the couple to dislodge the droplet.

In summary, when the initial surface oxide film is removed using CP (or destroyed in CH when very low oxygen partial pressures, p_{O2}, are used), acute θ ($\leq 90°$) is obtained even at low temperatures, which permits unhindered spreading. At high temperatures, the destruction of the oxide under vacuum lowers the θ[30,41] by 1) the formation of the volatile suboxide, Al_2O via the reaction: $4Al(l) + Al_2O_3(s) \rightarrow 3Al_2O(g)$, and 2) partial dissolution of Al_2O_3 skin in metal drop. These observations show that the positive effects of oxide removal (or low p_{O2}) could mask the negative effects of a low wettability test temperature. The effects of surface oxides are somewhat system-specific; surface oxides diminish the wettability (and joint strength) by obstructing the wettability-enhancing reactions in systems that are inherently reactive, but the oxide removal *per se* does not improve the wettability in non-reactive systems that are non-wettable.

In a manner similar to the Capillary Purification (CP) technique used in advanced sessile-drop tests, mechanical breakdown of oxides on the liquid front during infiltration under an applied pressure could also lower the θ and P_{th}. There are, however, fundamental differences between infiltration and CP. In CP, oxide is mechanically eroded due to the grinding action against the graphite syringe, whereas in pressure infiltration, external pressure would cause shear-thinning and film rupture via forced deformation of the oxide covering the liquid front.[42] Metal ingress occurs when the oxide ruptures. The modeling of these complex processes is difficult but a rough estimate of the pressure needed to fracture the oxide can be made by likening the film at the pore entrance as a symmetrically-loaded hemispherical elastic shell.[43] The two normal forces per unit length of the shell, N_θ and N_ϕ, can be obtained from the theory of elastic shells. Under a uniform pressure differential, ΔP, across a shell of thickness, y, these forces yield strain components whose maximum value (at $\phi = 41.8°$) are: $\varepsilon_{\phi(max)} = \Delta P d$

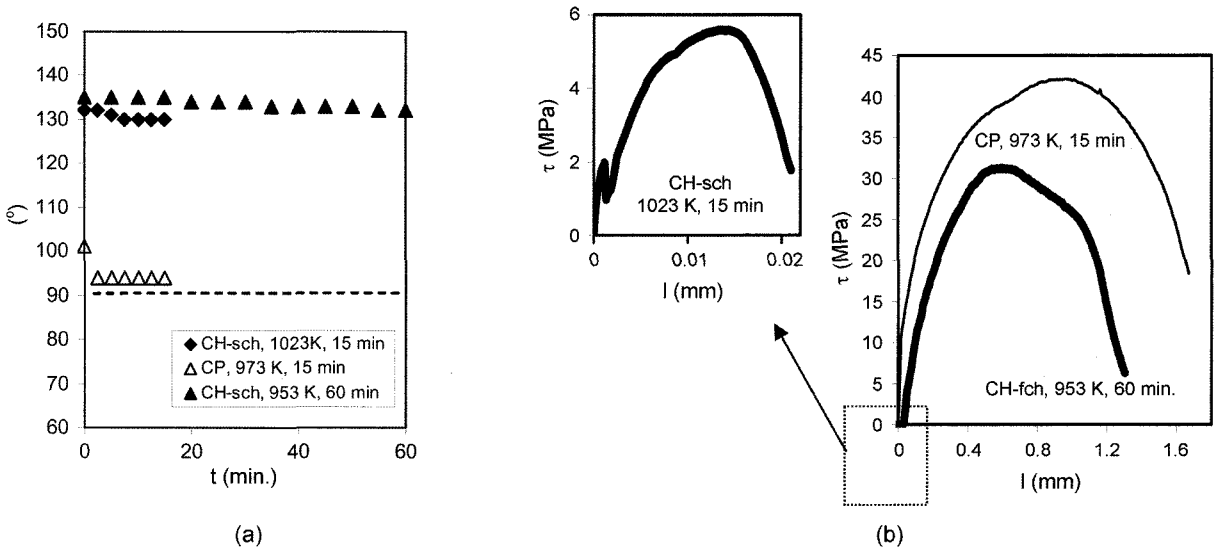

Fig. 3. Effect of contact heating (CH) and capillary purification (CP) on (a) wetting and (b) shear response of solidified sessile-drop couples of Al/Al_2O_3 (τ: shear stress).

$(4.668 + 0.668n)/8Ey$, and $\varepsilon_{\phi(max)} = \Delta Pd(0.668 - 4.448\nu)/8Ey$, where E and ν are the elastic modulus and Poisson's ratio of the oxide film, respectively, and d is the capillary (pore) diameter. If, it is assumed that the oxide ruptures when the product $E.\varepsilon_{\phi(max)}$ becomes comparable to the transverse rupture strength, σ, of the oxide, then the pressure to fracture the film may be estimated using handbook data for E, ν, and σ of Al_2O_3. Whereas the elastic shell analogy of the surface oxide (which is probably amorphous) is an idealization and fails to capture many essential aspects of the complex deformation processes, the estimated pressures are found to be comparable in magnitude to the measured threshold pressures in the SiC/Al system.[43]

2.3. Kinetics of Infiltration

2.3.1. Measurements

Infiltration kinetics of metals in porous ceramics have been measured using interrupted infiltration tests,[1,13-18,23,32,44-46] weight gain using thermogravimetry,[47-49] dynamic measurements using implanted electrodes,[50,51-53] and non-invasive capacitance methods.[20,29] Even for non-reactive systems, the flow kinetics in porous ceramics are influenced by a large number of variables, which include pore size distribution, pore shape, surface tension, contact angle, viscosity, density, magnitude of applied pressure (if used), rate of pressurization, metal temperature, composition, and gas atmosphere. Thermal properties may play a major role if the infiltration is non-isothermal and is accompanied by metal solidification.[54] Fig. 4 shows the influence of time on infiltration distance in some ceramic-metal systems. Infiltration increases with the contact time, and also with preform temperature and applied pressure.

For reactive systems, infiltration phenomenon is additionally affected by the structure and properties of freshly formed reaction product as well as by the mechanisms responsible for the system reactivity. Generally, Surface modification, matrix alloying or any other method applied to enhance the wettability will lead to faster infiltration. For example, wettable surface coatings and reactive alloying additions, which produce wettable reaction products, reduce the infiltration time and increase the infiltration length.

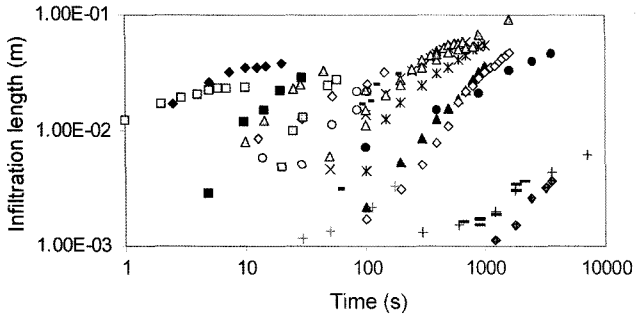

Fig. 4. Literature data on infiltration length versus time in SiC/Al, Al_2O_3/Al, SiO_2/Al, TiO_2+C/Al, AlN/Al, TiC/Al, and mullite/Al under different conditions of temperature, pressure and particle size.

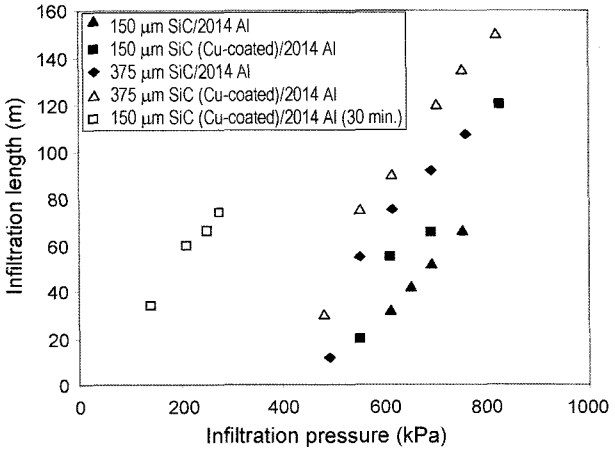

Fig. 5. Effect of Cu-coating on infiltration length in packed beds of single crystal SiC platelets, infiltrated by 2014Al alloy.

Even the surface-active alloying, which does not significantly improve the wettability (very small or negligible decrease in the contact angle value, which remains higher then 90°) but results in the reduction of the surface tension of the metal, there is a reduction in the pressure needed to overcome the capillary pressure resisting the flow in a non-wettable system. Many examples can be cited. Cu in Al slightly increases the P_{th} but Cu in the form of coating lowers the P_{th}[32] and permits greater infiltration lengths to be achieved in the SiC/Al composite (Fig. 5). In the case of Pb alloying of Al, Pb decreases the surface tension and threshold pressure for the infiltration of ceramics, and increases the infiltration length, even though Pb is non-reactive and it does not affect the contact angle value.[55] With Ti in Al/Al_2O_3, Ti alloying does not improve the wetting by Al but Ti coatings lower the θ.[36] Unlike Ti and Cu in Al, which do not improve the wettability as alloying additives, Cr is beneficial as both coating and alloying element in Ni/Al_2O_3 and Cu/Al_2O_3.[35,40,56,57] Other wettable coatings (Ni, Ag, Cr, K_2ZrF_6 etc) also lower the θ and P_{th} in ceramic/metal systems in all of which the dissolution of the coating in liquid metal is responsible for enhanced wettability. In the case of surface coatings of the compound K_2ZrF_6 used with Al or its alloys, the disruption of aluminum oxide film (which is partially dissolved by the fluoride species in the coating) presents an additional factor contributing to better wetting and consequent faster or deeper infiltration. The P_{th} decreases when K_2ZrF_6 is used but does not drop to zero.[46] Larger infiltration lengths are attained with K_2ZrF_6 coatings on ceramics. Similar effect of wettability improvement due to the oxide film disruption may be achieved by alloying Al with Mg, that along with lowering of σ_{lv} contributes to reduction P_{th}.[17]

Even at slow spreading rates characteristic of low (<1 MPa) pressure gas infiltration techniques, spreading could be faster than coating dissolution so the infiltrating liquid is constantly exposed to a wettable (coated) surface, thus enhancing the infiltration. At higher pressures

(squeeze casting), where flow is faster (~1 $m \cdot s^{-1}$), infiltration is completed prior to coating dissolution, and residual coatings on particle surface could remain after solidification (often as exfoliated or partially cracked surface layers).

2.3.2. Theory

Two fundamentally different approaches are used to model infiltration: Darcy's equation which yields an averaged flow behavior, and fluid physics based models that solve the equation of fluid motion in a single pore (capillary). For steady-state unidirectional flow, Darcy's equation is $u = -\frac{\kappa dp}{\mu dx}$, where u is the velocity, p is the pressure, μ is the dynamic viscosity of the fluid, κ is the permeability of the porous medium which is intimately related to void fraction and pore size distribution. Empirical relationships to predict the permeability of packed beds of particulates and fiber bundles, including geometrical correction factors for shape deviation from perfectly spherical, and for misalignment of the fibers, have been derived. However, the complexity of real porous solids renders theoretical predictions somewhat difficult if not unreliable, with the result that k is generally determined with the aid of Darcy's law and from experimental measurements of fluid velocity and pressure gradient. This renders the entire approach somewhat circuitous, and of limited value. The second theoretical approach develops an equation of fluid motion within a single idealized pore in terms of the various forces acting on the fluid. For counter-gravitational (rise) of a wettable liquid in a straight cylindrical capillary of radius R, the fluid motion can be described by the following differential equation that includes surface tension, viscous drag, end drag and gravitational forces,[58,59]

$$2\pi R\sigma_{LV}\cos\theta - \pi R^2\rho gh - 8\pi\mu h\frac{dh}{dt} - 0.25\pi R^2\rho\left(\frac{dh}{dt}\right)^2 = \frac{d}{dt}\left[\pi R^2 h\frac{dh}{dt}\right] \quad (1)$$

where σ_{LV} is surface tension, ρ is density of melt, θ is (equilibrium) contact angle, μ is viscosity, is acceleration due to gravity and h is the infiltration distance. This equation can be rewritten as

$$h\left(\frac{d^2h}{dt^2}\right) + 1.25\left(\frac{dh}{dt}\right)^2 + ah\left(\frac{dh}{dt}\right) + gh = b \quad (2)$$

where $a = \frac{8\mu}{\rho R^2}$ and $b = \frac{2\sigma_{LV}\cos\theta}{\rho R}$. This non-linear equation can be solved numerically subject $h = \left(\frac{dh}{dt}\right) = 0; t = 0$ to the initial conditions to derive the kinetics of capillary rise. A few limiting cases of practical interest that permit analytical solution can also be envisioned. For example, if the acceleration term is small, then the following solution to Eq. (2) is obtained

$$h^2 = \left[\frac{R\sigma_{LV}\cos\theta}{2\mu}\right]t - \left[\frac{\rho ghR^2}{4\mu}\right]t - \frac{\rho^2R^4}{32\mu^2}\left[\exp\left(\frac{-8\mu t}{\rho R^2}\right) - 1\right] \quad (3)$$

At slow rate of rise and negligible end drag, an asymptotic solution, or the Washburn equation is obtained, which represents the long-time, steady-state solution. This equation has the form

$$h^2 = \left(\frac{\rho R^2}{4\mu}\right)\left[\frac{2\sigma_{LV}\cos\theta}{\rho R} - gh\right]t \quad (4)$$

If the total penetration length, h, is much smaller than the height, h_{eq}, to attain hydrostatic equilibrium (i.e., $h << h_{eq}$, where $h_{eq} = 2\sigma_{LV}\cos\theta/\rho gR$), then

$$h\frac{dh}{dt} = \frac{\rho R^2}{4\mu}\left(\frac{\sigma_{LV}\cos\theta}{\rho R}\right) \quad (5)$$

and the solution becomes a particularly simple parabolic expression

$$h^2 = \left(\frac{R\sigma_{LV}\cos\theta}{2\mu}\right)t \quad (6)$$

If the capillary radius is small, the infiltration length depends mainly on the parameter ($R\sigma_{lv}\cos\theta/2\mu$); larger the value of this parameter, greater is the infiltration distance in a given time. Thus, the simplest capillary-rise model yields a parabolic increase in infiltration distance, h, with time.

The parabolic solution has been applied to infiltration of metals in porous sintered alloys such as Fe-Cu, Fe-Ag, Cu-Ag, Cu-Pb, Fe-Pb, Cu-Sn, Sn-Pb, Ni-Ag, and porous TiC compacts infiltrated with Al. The expression for the parabolic infiltration kinetics ($h^2 = kt$) shows that the parameter ($r\sigma_{lv}\cos\theta/2\mu$) can be considered as an infiltration rate constant, k. The experimental data on the effect of t on h in several oxide and carbide ceramics[13,25,42,44,47,50,60-63] were shown in Fig. 4. Usually, quantitative agreement between theory and experiment is not achieved due to several reasons. Discrepancies arise even in wettable systems, and may be due to both hydrodynamic and interfacial factors, which include irreversible losses due to sudden expansion/contraction of pores, unsteady multidirectional flow, uncertainties in the effective pore radius, increase in physical and chemical inhomogeneity of the ceramic surface, and transient capillary forces due to temporal evolution of the contact angle.

2.3.3. Infiltration Rate Constant and Activation Energy

Assuming parabolic kinetics ($h^2 = Kt$) for infiltration, the approximate values of the infiltration rate constant, k, given from $k = R\sigma_{LV}\cos\theta/2\mu$, can be extracted from the experimental measurements of infiltration kinetics. Experimental values of k are displayed in Fig. 6 for SiC/Al and Al_2O_3 (Safil)/Al composites based on data from different studies;[12,13,42,50,61] the data show that k varies roughly between 4.4 $mm^2 \cdot s^{-1}$ to 1428 $mm^2 \cdot s^{-1}$. The measured infiltration rate constants for infiltration of sintered compacts show that (k_{theor}/k_{exp}) could vary from less than 10 to over 60. Such large discrepancy has been attributed chiefly to the assumption of a constant contact angle[64] as discussed later. Wettable coatings increase the k; for example, Cu coatings on SiC increased

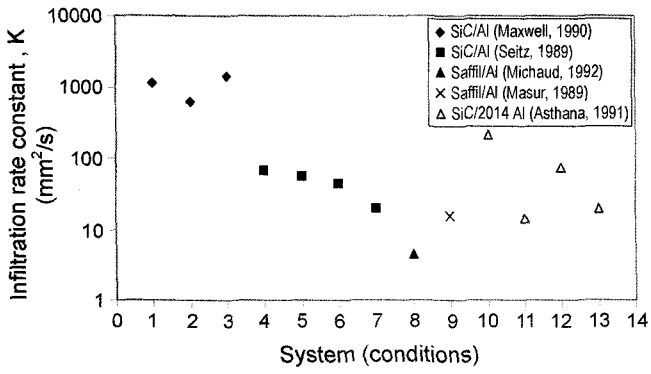

Fig. 6. Infiltration rate constant ($R\sigma_{lv}\cos\theta/2\mu$) for SiC and saffil (alumina short fibers) infiltrated with molten Al.

the k for Al infiltration from 72.3 to 213.2 $mm^2 \cdot s^{-1}$. The value of k for powder metal parts[10,64] is generally 174 – 812 $mm^2 \cdot s^{-1}$. For a large number of high-temperature systems, the rate constant k varies with temperature, T, according to the Arrhenius relationship $k = A\exp(-Q/RT)$, where Q is an activation energy. The flow is thus thermally-activated, and the value of Q is suggestive of the dominant transport mechanisms driving the flow. Typical Q value for SiC/Al[42] is 58.8 $kJ \cdot mol^{-1}$, for TiC/Al[48] it is 105.0 – 445 $kJ \cdot mol^{-1}$ for 1 – 25 mm pores, and for the reactive penetration (section 4) of dense and porous mullite with Al,[60] it is 70 and 185 $kJ \cdot mol^{-1}$, respectively. Transitions in operative mechanisms, reflected in the Q value, occur with changes in T and/or pore radius, R (e.g., due to exothermic reactions, pore shrinkage or expansion due to product phase deposition or ceramic dissolution, etc.). For example, in TiC/Al,[48] infiltration is limited by atomic diffusion at small R, and by interface reaction kinetics at large R. This occurs because with increasing pore radius, R, the liquid volume in the capillary increases faster than the solid's surface area, which triggers reaction control and slower infiltration due to reduced supply of reactive species by the solid. However, at small R, shallow solute gradients develop and flow begins to be limited by diffusion.

3. Reactive Infiltration

In reactive infiltration, the reinforcing phase can form via a chemical reaction. The reaction is usually exothermic (e.g., infiltration of silicon in porous carbon, and infiltration of aluminum in TiO_2, mullite ($3Al_2O_3 \cdot 2SiO_2$) and in Ni-coated alumina). The infiltration conditions can be controlled to achieve the desired level of conversion and structure. The reactive infiltration of Si in porous C forms reacted SiC phase and unreacted C in a Si matrix. Preexisting SiC grains are employed as inert filler in the porous C preform to permit heterogeneous nucleation and bonding of SiC. The porous perform is made by pyrolyzing a high-char polymer precursor material, and some control on pore size, volume fraction and morphology is possible. Reactive infiltration can produce two or more phases via chemical reactions with a suitable choice of the precursor materials. For example, both TiB_2 and AlN phases form by reactive spontaneous infiltration of TiN, TiC_xN_{1-x}, and B powders with AlMg alloys.[65] Low values of x yield a greater quantity of product phases. The infiltration rate in this system is controlled by the strongly exothermic reaction: $TiN + 2B + Al \rightarrow AlN + TiB_2$. In this case, the heat of reaction depends upon the magnitude of x; low values of x lead to higher heat of reaction and faster infiltration rates whereas high values of x lead to low heat of reaction and slower infiltration. The highest infiltration rates are achieved when TiN, B and AlMg are used as starting materials. The presence of Mg is necessary for self-infiltration in this system as in many others.

3.1. Kinetics of Reactive Infiltration

3.1.1. Measurement

In an early work, Einset[53] attempted to measure the infiltration front velocity of molten Si through thin tapes of carbon performs containing SiC particles as a function of temperature. Thermocouples were inserted along different points in the tape to record the temperature rise due to the strong exothermic C/Si reaction. A major drawback of these measurements was that Si traversed the path of least resistance (outer surface of the tape) rather than through the fine tortuous channels within the perform. In a later work, Sangsuwan *et al.*[51] inserted thermocouples within porous carbon performs to track the liquid front and record the temperature rise. The peak temperatures showed a decrease with increasing distance from the bottom surface of the perform exposed to molten Si. This indicated a progressive decrease in the infiltration front velocity with increasing distance, which is consistent with the behavior predicted the parabolic solution to the capillary rise model. The numerical discrepancy between the capillary rise model and the measured velocity is, however, nearly two orders of magnitude. It thus appears that the capillary flow model must be modified to include the reaction kinetics which appears to be driving the flow in the Si/C system.

Two basic mechanisms for the reaction of C and Si have been proposed.[66,67] In the first, a thin film of SiC forms on the carbon surface, through which Si and C diffuse (possibly along the grain boundaries in SiC), and cause continued reaction and conversion to SiC. The nearly 58% volumetric expansion upon conversion of C to SiC may cause the freshly formed SiC layer to spall off, exposing fresh carbon to Si. This exposure is believed to result in the dissolution of C in Si, saturation of Si with C, and reprecipitation of SiC, followed by SiC grain coarsening via competitive dissolution and growth (Ostwald ripening). Thus, in the first mechanism, the reaction kinetics are either controlled by the inward diffusion of Si through the reaction-formed SiC layer, which is the basis of the 'shrinking core' model,[68] or by the outward diffusion of carbon through the SiC layer, which is the basis of the 'bulging core' model. In the second mechanism proposed for the reaction of C and Si (the dissolution-reprecitation mechanism), the dissolution of C in Si,

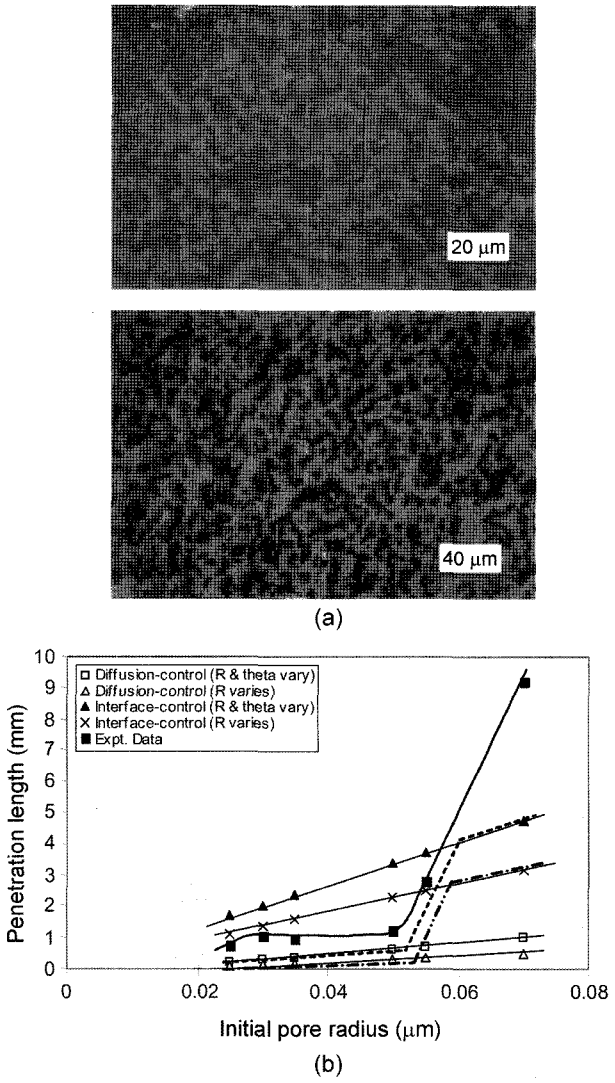

Fig. 7. (a) Microstructure of porous carbon performs infiltrated with molten Si, and (b) comparison of measured penetration distance of Si in porous C (initial pore size R_0=10 μm) from ref. [51] and theoretical predictions. Data for pore radii <0.05 μm are from sessile drop tests on carbon substrate from ref. [70].

and diffusion to cooler regions in the melt is believed to be responsible for the precipitation of SiC which may undergo coarsening. A correlation between the temperature-dependence of carbon solubility in Si at short times and the initial SiC growth rate was used to support this mechanism. An analysis of the Si/C reaction kinetics data reveals[69] that the Si diffusion through the SiC layer is the more likely reaction mechanism operative during porous carbon infiltration by molten Si. Fig. 7(a) shows the microstructure of a porous carbon perform infiltrated with molten Si, and Fig. 7(b) shows the maximum penetration distance of molten Si in carbon performs as a function of the effective pore radius. This figure also shows theoretical results based on different assumptions concerning the reaction of Si with C during infiltration. The data for radii less than 0.05 μm in Fig. 7(b) are from the measurement of penetration distance of sessile drops of molten Si in the carbon substrates underneath the droplets;[70] these measurements, therefore, represent the effect of a finite size Si reservoir (droplet) on the maximum infiltration distance, which is different from conventional infiltration (rest of the data in Fig. 7(b)) in which virtually an inexhaustible supply of Si is in contact with the microporous carbon performs. Fig. 7(b) shows that the calculations are only qualitatively in agreement with the experimental results. Possible sources of discrepancy are discussed in Sec. 3.1.3.

3.1.2. Theory

Models of reactive infiltration consider pore size evolution during infiltration, and invoke the concept of a variable preform permeability $\kappa(t)$, which varies with both time t and spatial coordinate l. The specific functional dependence of k on l and t is determined by both the initial pore structure, and the microscopic reaction kinetics and deposition morphologies (e.g., formation of a continuous reaction layer versus discontinuous deposition of product phase). For the simpler case of a permeability that is a function of time alone, the problem has been solved in analytic form.[71] If the pores of radius R shrink with either linear or parabolic time dependence, as may be appropriate for interface-controlled and diffusion-controlled reaction kinetics, respectively, then $R(t) = R_0 - kt$ and $R(t) = R_0 - k_1\sqrt{t}$, where k and k_1 are linear and parabolic rate constants, respectively. The corresponding infiltration distance versus time relationships are obtained from integration of an appropriate fluid flow model. For a simple capillary rise model that assumes parallel capillaries of identical diameter, the permeability $\kappa(t)$ is given from $\kappa(t) = PR^2/8$, where P is the pore volume fraction. For more complex geometries, hydraulic radius is used; this changes only the numerical constant in the expression for permeability but not the parabolic dependence on pore radius (R^2 dependence). Assuming that geometry of the pore does not change during infiltration and reaction, the time-dependent permeability for the reactive infiltration is obtained from the temporal evolution of pore radius as aresult of the reaction. Thus, for the Hagen-Poiseulle model, $\frac{\kappa(t)}{W_0} = \frac{R^4(t)}{8R_0^2} = \beta R^4(t)$, where W_0 is the initial porosity. Here $R(t)$ is given from linear (interface-controlled) or parabolic (diffusion-controlled) rate expressions. Using these expressions in Darcy's equation and integrating the resulting equation yields the solutions for infiltration kinetics for interface-controlled and diffusion-controlled cases, respectively, as[71]

$$h^2(t) = \frac{2\beta\Delta P}{\mu}[R_0^4 t - 2R_0^3 k t^2 + 2R_0^2 k^2 t^3 - R_0 k^3 t^4 + 0.2k^4 t^5] \quad (7)$$

$$h^2(t) = \frac{2\beta\Delta P}{\mu}\left[R_0^4 t - \frac{8}{3}R_0^3 k_1 t^{1.5} + 3R_0^2 k_1^2 t^2 - \frac{8}{5}R_0 k_1^3 t^{2.5} + 0.33 k_1^4 t^3\right] \quad (8)$$

where β is a geometric factor given from $\beta = (8R_0)^2$. Of cen-

tral importance to the final dimensions of the component to be processed is the final infiltration length h_f, at which reaction choking will occur. This limiting length for interface-controlled and diffusion-controlled cases is given from $h_f = \sqrt[4]{\frac{2\beta\Delta P R_0^5}{5\mu k}}$ $h_f = \sqrt[6]{\frac{2\beta\Delta P R_0^6}{15\mu k_1^2}}$, respectively. Only qualitative assessment of these equations against experiments has been attempted; for example, the model predicts the fast infiltration rates observed experimentally, and shows that limiting infiltration depth is achieved literally in seconds. For fine-scaled carbon microstructure with fine pore size, the time to complete the reaction is only on the order of seconds for the appropriate values of reaction rate constants k and k_1. More rigorous numerical models of the reactive infiltration phenomenon have been developed;[69,72,73] these models either treat isothermal infiltration with reaction and ignore the strong exothermic effects of the Si/C reaction or treat the infiltration as unidirectional, both of which limit their applicability to real systems.

The limiting depth, h_f, is increased by external pressure, by increasing the pore size, or by decreasing the reaction rate. Preforms can be designed to control the pore size, pore volume fraction and pore morphology. The pore size determines the solute concentration gradient; the solutes released at the reaction front should be able to diffuse into the liquid for reaction and flow to continue. In the event of a high transient solute build up, further solute rejection is slowed down to match the rate at which the released solute can diffuse away. A high solute concentration at the reaction front will also retard the reaction because of reduced thermodynamic driving force. If the pore size is increased, solute diffusion becomes easier since metal sink becomes larger in size and can accommodate a larger quantity of solute; as a result, a larger concentration gradient is created. If, however, interface reaction rather than solute diffusion is controlling the infiltration, then as the pore size is increased, the effective surface area of the ceramic phase decreases; this in turn limits the supply of the reactant species in the solid (e.g., in TiO_2-Al, an increase in the TiO_2 pore size reduces the available oxygen[49]). As a result, reaction rather than diffusion begins to control the infiltration. Attempts to increase the limiting length may be hindered by reaction choking, product spallation and pore closure. The volume changes that accompany chemical reactions due to different specific volumes of reactant and product phases give rise to considerable stresses and distortion and crack formation.

3.1.3. Role of Transient Wetting

In reactive infiltration, pore size may constantly change due to specific volume changes caused due to chemical reactions. In addition, the angle θ usually exhibits a protracted time-dependence, and could take a long time to stabilize at its equilibrium value, θ_∞, even in wettable systems. Both time-dependent pore radius, $r(t)$, and the contact angle, $\theta(t)$, modulate the capillary forces that drive the infiltration. The experimentally measured contact angle θ usually decays with time according to[74,75] $\theta(t) - \theta_\infty = (\theta_0 - \theta_\infty)\ \exp(-t/\tau)$, where θ_0 is the contact angle at zero time, and τ is a characteristic time of the system. As far as reactions are concerned, two limiting situations can be envisioned:[71,76] reaction limited by interface processes (attachment kinetics) and by diffusion processes. For diffusion- and interface control, respectively, parabolic ($R(t) = R_0 - m\sqrt{t}$) and linear ($R(t) = R_0 - kt$) kinetics can be expected, where m and k are the appropriate reaction rate constants. These expressions can be incorporated in capillary rise models for inert liquids (e.g., Washburn equation) to derive the isothermal capillary rise kinetics under diffusion- and interface control with a time-dependent contact angle.[77-80] Representative computational results are discussed below.

During infiltration of porous carbon by molten Si,[51,81] SiC formation causes a 134 pct. volumetric expansion, resulting in pore shrinkage. The $\theta - t$ data for Si/C at 1755 K[82] were fitted to $\theta(t) - \theta_\infty = (\theta_0 - \theta_\infty)\ \exp(-t/\tau)$, and the baseline values of the reaction rate constants were taken to be[71,76] $k \approx 4 \times 10^{-8}\ \mathrm{m \cdot s^{-1}}$ and $m \approx 2 \times 10^{-7}\ \mathrm{m \cdot s^{-1/2}}$. Computations show (Fig. 8(a)) that for Si in porous C ($R_0 = 10$ mm), the Washburn equation overestimates the flow kinetics in qualitative

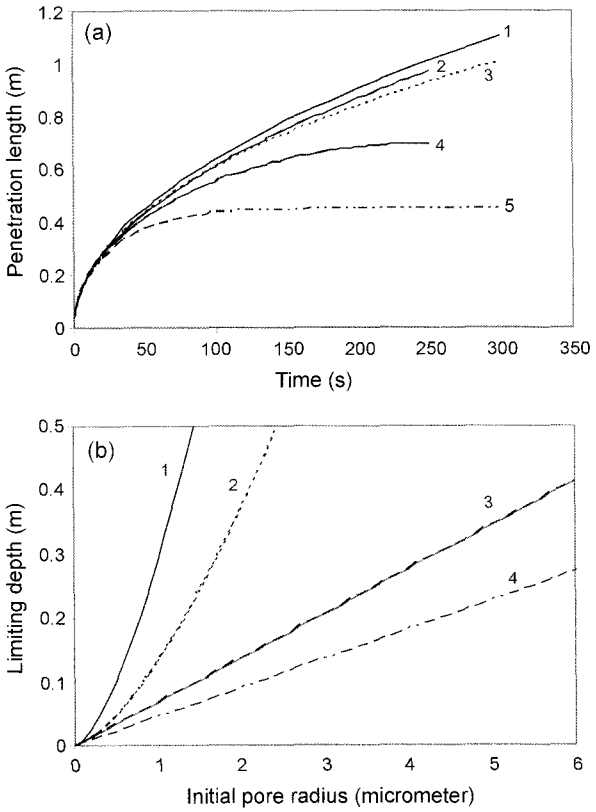

Fig. 8. (a) Infiltration profiles for Si/C (R_0=10 μm). *Curve (1)*: Washburn eq.; *curve (2)*: diffusion-control, *curve (3)*: diffusion-control (constant θ), *curve (4)*: interface-control, *curve (5)*: interface-control (constant θ); and (b) limiting length versus R_0 for Si/C: *Curve (1)*: diffusion-control, *curve (2)*: diffusion-control (constant θ), *curve (3)*: interface-control, *curve (4)*: interface-control (constant θ).

agreement with the experiments[51] in which the measured velocity of Si in C was smaller than the Washburn velocity. Calculations also show[77] that for both interface- and diffusion-limited flow, penetration lengths are larger when both θ and R vary with time than when R is allowed to decrease but the capillary pressure is constrained to remain constant (as was done in ref. [71]). The limiting lengths (typically, a few mm) due to reaction choking (Fig. 8(b)) increase with R_0, and are larger when both θ and R vary than when only R decreases but θ remains constant. In both cases, diffusion-limited flow is faster than interface-limited flow as would be expected from the slower product phase growth under diffusion-control.

Although the preceding results physical insights into reactive infiltration, several factors render quantitative predictions somewhat uncertain. For example, reliable values of the reaction rate constants, m and k, are difficult to obtain at the process temperature, and the exothermicity of the reaction, ignored in the calculations, can strongly influence the infiltration. The temperatures could rise by 390° to 740° above the melting point of Si,[51] which will alter the melt properties and the infiltration behavior. In addition, q values could deviate from an exponential function (at $t \sim 0$), and be sensitive to the actual test conditions (p_{O2}, T, alloying, etc.).[30,83] Also, transitions in the reaction mechanisms (interface-control versus diffusion-control) are seldom abrupt, and mixed control may be operative during the flow, which is not accounted for in the preceding calculations. The compositional changes due to reactions alter the melt properties and diffusivity, and the morphological features and defect structure (porosity, grain boundaries) of the interface interphases influences the extent of chemical attack via short circuit paths.

Finally, discrepancies between the theory and the measurements could be caused by a dynamic contact angle. It is well-known that the angle θ is distorted at high velocities due to hydrodynamic effects, resulting in a modulation of the capillary forces. In inert (organic) liquids, θ exhibits velocity dependence above $\sim 10^{-4}$ m·s^{-1}.[84] The observed velocity, U, of Si in porous C (median pore dia ~ 1.25 mm) is in the range[51] $\sim 0.5 \times 10^{-3}$ to 4.5×10^{-3} m·s^{-1}, which suggests that a dynamic θ may become important in this case. Models to predict the effect of U on θ in reactive systems are non-existent. As a first step, classical models[6,85-87] for inert liquids can be examined in the context of reactive flow. A model due to De Gennes[85] shows that the effect of fluid velocity on contact angle can be modeled by $U = C(\sigma_{lv}/\mu)\theta^m$, where C is a constant (~0.02 rad^{-3}) and $m \sim (3 \pm 0.5)$. Others have either developed empirical θ-U relationships[6,87] or presented surface physics models[86] that consider sliding of the molecules along the solid's surface from the liquid to the vapor side of the interface.

The projections of infiltration kinetics were made[78] by incorporating the De Gennes model[85] in the Washburn equation. These were compared with the experimental results for Si/C from ref. [51]. The unmodified Washburn

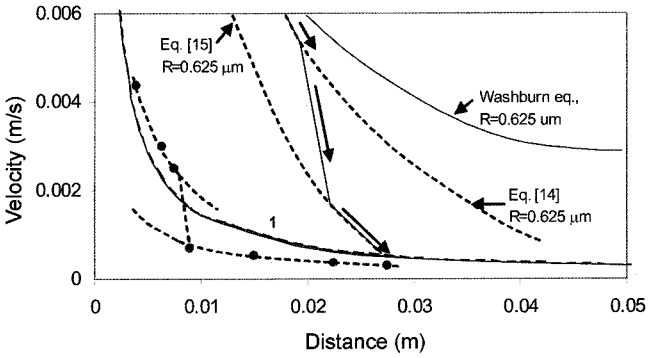

Fig. 9. Comparison of velocity of Si in porous C reported in ref. [51] and theoretical predictions. *curve 1:* outcome based on the De Gennes model, *curve 2:* diffusion-control (variable R and θ), and *curve 3:* interface-control (variable R and θ). The dashed curves show possible paths when a transition from diffusion-driven flow to reaction-driven flow occurs with increasing infiltration distance.

equation (for a median pore dia of 1.25 μm) yields large discrepancy as noted in Fig. 9. In contrast, the De Gennes model (curve 1, Fig. 9) seems to yield a reasonable agreement with the velocity data of ref. [51] when an effective (rather than median) pore dia of 0.14 μm was used. However, this model fails to predict the observed abrupt drop in the velocity in Si/C. The measured velocity of Si in porous C preforms of median pore dia ~ 1.25 μm, shown in Fig. 9, exhibits an abrupt drop of ~ 73 pct. over an infiltration distance, h, of 0.007 – 0.009 m. This drop is believed to be the result of a transition in the mechanisms driving the capillary flow; at short distances, flow is limited by interface reactions and at large distances, flow is limited by the diffusion of Si and C through the SiC product phase. This is consistent with the calculations presented in ref. [78]; the resulting behavior is seen to qualitatively mimic the observed drop even though the numerical magnitude of the discrepancy between the theory and measurements is quite large. The calculation, therefore, captures the basic elements of the physics, but needs refinement for actual quantitative use.

4. Reactive Metal Penetration

Reactive penetration refers to metal ingress in dense ceramics (single crystals, fully dense polycrystals, amorphous ceramics, etc) which are devoid of pre-existing porosity. The liquid advance is controlled by the movement of the reaction front which reconstructs the contacting interface. In both infiltration and penetration, chemical reactions form an interpenetrating network of metal and ceramic crystals (e.g., Al and Al_2O_3). For example, such structures form in single crystal ZnO (ZnO^{SC}), where there are no grain boundaries, and in amorphous SiO_2 and fully-dense mullite and fly ash when they are in contact with molten Al.[37,88-92] It is interesting to note that reactive penetration occurs (and

an interpenetrating Al-Al_2O_3 structure forms) in dense ceramics like ZnO, which are not wet by Al, but Al does not spontaneously infiltrate porous TiO_2 and ZrO_2 even though these ceramics are wetted by Al. Similar anomalies are observed in porous ceramics. For example, when porous carbon is in contact with Cu-Ti or Cu-Cr alloys, TiC or Cr_3C_2 form.[93,94] It is observed[93] that the TiC reaction layer in Cu-Ti/C does not prevent melt penetration of porous carbon (even though $\theta > 90°$), but Cr_3C_2 reaction layer in Cu-Cr/C hinders melt impregnation even though the measured contact angle, $\theta < 90°$. Most observations of reactive penetration are based on the sessile-drop wettability tests in which metal penetration of the underlying substrate is observed. Substrate cracking due to chemical transformations may contribute to better infiltration whereas secondary oxidation of the metal will increase the resistance to penetration.

Reactive penetration of dense (and amorphous) fly ash by Al forms fine Al_2O_3 crystals, while concurrently enriching molten Al with Si and Fe released from the dissolution of fly ash in Al. In a broader sense, the S/L interactions may not always lead to the creation of a new product phase, and new crystals of a preexisting phase may nucleate and grow by a dissolution-re-precipitation process. For example, fine Al_2O_3 crystals form in non-reactive Al/Al_2O_3 at the S/L interface underneath sessile drops as confirmed by the microscopic examination of the interfaces in solidified sessile drop couples.[35,88,95] The new Al_2O_3 crystals at the S/L interface form by the dissolution of the Al_2O_3 substrate, saturation of the melt with O, and re-precipitation of new Al_2O_3 crystals which grow epitaxially on the interface. In addition, O diffusion along S/L interface may also aid the formation of these crystals.[95] These micro-crystals strengthen the joint.

Reactive penetration in Al/TiO_2 and Al/mullite occurs[37,38] in a manner similar to Al/flyash. Fig. 10 shows views of sessile drop test samples of Al in contact with titania and mullite substrates, and the appearance of the penetration layers. Detailed microstructural examination has shown that in sessile drops of Al on TiO_2 at $T \geq 1173°K$,[38] new Al_2O_3 crystals form at the interface surrounded by Ti-rich Al. On the drop-side of the interface, large Al_2O_3 crystals form by dissolution-precipitation, and on the substrate side, very fine Al_2O_3 crystals, surrounded by an Al impregnated region, form. At even higher temperatures (≥1373°K), Al wets, reacts, and penetrates the TiO_2, forming a continuous network of Al_2O_3 crystals interpenetrated by a continuous Al network. The governing reaction is $4Al(l) + 3TiO_2 \rightarrow 2Al_2O_3 + 3Ti$. The penetration layer in Al/TiO_2 attains a thickness of a few micrometers (e.g., 2 – 8 mm at 1273°K in 30 min. contact). TiO_2 reacts with Al to form Ti aluminides via the reaction $TiO_2 + Al \rightarrow Al_2O_3 + Al_xTi_y$, where the type of aluminide (e.g., Ti_3Al, TiAl, $TiAl_3$) formed depends upon the TiO_2/Al ratio. Thus, wettability improvement in Al/TiO_2 is due to the formation of a favorable interface structure from the preceding chemical reactions.

The penetration behavior in Al/SiO_2 is also reaction-assisted,[37,39] promoted by the reaction $4Al(l) + 3SiO_2 \rightarrow 2Al_2O_3 + 3Si$. The reaction product layer (RPR) plays an important role in aiding or impeding the spreading and flow. Sessile-drop tests show[37] that cracking of SiO_2 near the triple line (TL) (due to expansion accompanying $SiO_2 \rightarrow Al_2O_3$ transformation) does not hamper the RPR propagation, and the RPR is able to advance beyond the TL. Alloying Al with Si does not change the preceding reaction between Al(l) and SiO_2, but reduces the reactivity, and leads to poor wetting. In contrast, with Ti alloying of Al, the contact angle in the SiO_2/Al couples rapidly decreases, and Si (from the preceding chemical reaction) reacts with Ti to form titanium silicide ($TiSi_2$) via the reaction $Ti + 2Si \rightarrow TiSi_2$.

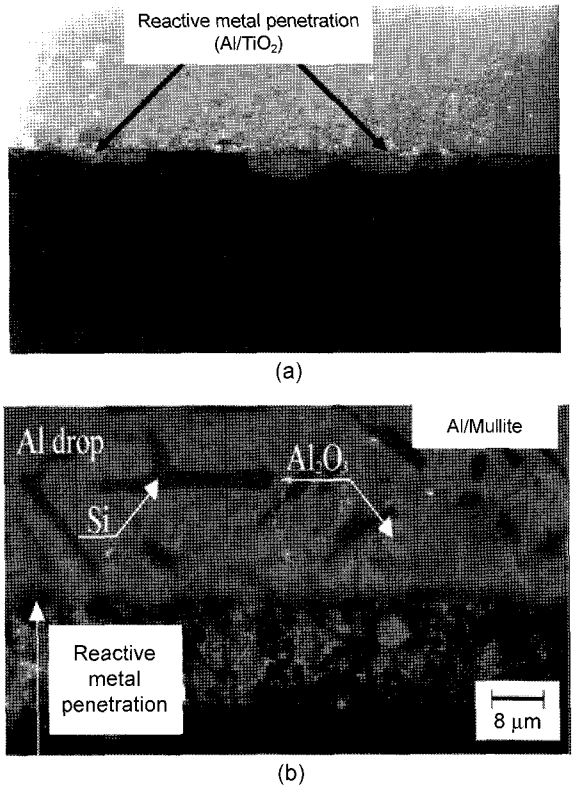

Fig. 10. Reactive metal penetration underneath sessile drops of Al on (a) a TiO_2 substrate, and (b) a mullite substrate.

5. Reactive Infiltration and Ceramic Joining Technology

Reactive infiltration has been profitably used in an innovative joining technology for ceramics, in particular silicon carbide ceramics.[96-99] The basic joining steps include the application of a carbonaceous mixture in the joint area and curing at 383 – 393°K for 10 – 20 min. Silicon in paste form is applied in the joint region and heated to 1698°K C for 5 – 10 min. The molten Si reacts with carbon to form silicon carbide with controllable amounts of residual silicon at the joint. Fig. 11 shows the interface region of reaction-bonded (RB)-SiC, and sintered SiC joints, produced by Si infiltra-

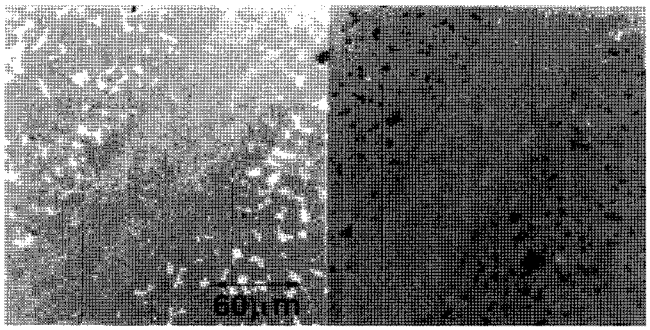

Fig. 11. Joining of SiC using reactive infiltration. (a) reaction-bonded (RB)-SiC, and (b) sintered SiC joints, produced by Si infiltration of a carbonaceous mixture applied to the SiC/SiC joint. The white and gray areas in (a) and (b) are Si and SiC, respectively.

tion of a carbonaceous mixture that was applied at the mating surface of the joints. The method has been used to join different types of SiC such as reaction-bonded and sintered. The thermomechanical properties of the joint interlayer can be tailored close to those of the silicon carbide-based matrix materials, and high-temperature fixturing is not needed to hold the parts at the high temperatures required for infiltration.

6. Conclusions

Features of reactive infiltration of porous ceramics by liquid metals to fabricate ceramic-metal composites were described. In particular, the complex role of interfacial reactions, oxidation of the metal front, pore modulation and closure due to reactions, and a transient contact angle were discussed with examples from widely studied ceramic/metal systems. Possible theoretical effects of these phenomena on infiltration were discussed together with the experimentally observed behavior. In addition, chemical and structural changes accompanying the reactive penetration of dense ceramics (e.g., single crystals, amorphous ceramics etc.) by molten metals upon prolonged contact was also discussed.

Acknowledgement

R. Asthana thankfully acknowledges a NASA SFRO award during June-Aug 2005.

REFERENCES

1. C. Garcia-Cordovilla, E. Louis, and J. Narcisco, "Pressure Infiltration of Packed Ceramic Particulates by Liquid Metals," *Acta Mater.*, **47** [18] 4461-79 (1999).
2. R. Asthana, *Solidification Processing of Reinforced Metals*, Trans Tech, Switzerland (1998).
3. E. J. Gonzalez and K. P. Trumble, "Spontaneous Infiltration of Alumina by Cu-O Alloys," *J. Am. Ceramic Soc.*, **79** [1] 114-20 (1996).
4. V. Kevokijan, "Mg AZ80/SiC Composite Bars Fabricated by Infiltration of Porous Ceramic Preforms," *Metall. Mater. Trans.*, **35A** 707-15 (2004).
5. A. Lorenz, E. Sachs, S. Allen, L. Rafflenbeul, and B. Kernan, "Densification of a Powder Metal Skeleton by Transient Liquid-Phase Infiltration," *Metall. Mater. Trans.*, **35A** 631-40 (2004).
6. P. Van Remoortere and P. Joos, "About the Kinetics of Partial Wetting," *J. Colloid Interface Sci.*, **160** 387-96 (1993).
7. J. Szekely, A. W. Neumann, and Y. K. Chuang, "The Rate of Capillary Penetration and the Applicability of the Washburn Equation," *J. Colloid Interface Sci.*, **35** [2] 273-78 (1971).
8. M. Letelier, H. J. Leutheusser, and C. Rosas, "Refined Mathematical Analysis of the Capillary Penetration Problem," *J. Colloid Interface Sci.*, **72** [3] 465-70 (1979).
9. J. P. Ligenza and R. B. Bernstein, "The Rate of Rise of Liquids in Fine Vertical Capillaries," *J. Am. Chem. Soc.*, **73** 4636-38 (1951).
10. K. A. Semlak and F. N. Rhines, "The Rate of Infiltration of Metals," *Trans. AIME*, **21** 325-31 (1958).
11. S. Y. Chong, H. V. Atkinson, and H. Jones, "Effect of Ceramic Particle Size, Melt Superheat, Impurities, and Alloy Conditions on Threshold Pressure for Infiltration of SiC Powder Compacts by Aluminum-Based Melts," *Mater. Sci. Eng.*, **A173** 233-37 (1993).
12. P. B. Maxwell, G. P. Martins, D. L. Olson, and G. R. Edwards, "The Infiltration of Aluminum into Silicon Carbide Compacts," *Metall. Trans.*, **21B** 475-85 (1990).
13. R. Asthana and P. K. Rohatgi, "Melt Infiltration of SiC Compacts. Part I: Study of Infiltration Dynamics', and 'Part II: Evaluation of Solidification Microstructures," *Z. Metallk.*, **83** [12] 887-92 (1992), and **84** 44-7 (1993).
14. S. Y. Oh, J. A. Cornie, and K. C. Russel, "Wetting of Ceramic Particulates with Liquid Aluminum Alloys: Part I. Experimental Techniques', and 'Part II. Study of wettability," *Metall. Trans.*, **20A** 527-32 and 533-41 (1989).
15. J. Narcisco, C. Garcia-Cordavilla, and E. Louis, "Pressure Infiltration of Packed Alumina Particulates by Pure Silver," *Scripta Mater.*, **36** [4] 363-68 (1997).
16. E. Candan, H. V. Atkinson, and H. Jones, "Role of Surface Tension in Relation to Contact Angle in Determining the Threshold Pressure for Melt Infiltration of Ceramic Powder Compacts," *Scripta Mater.*, **38** [6] 999-1002 (1998).
17. E. Candan, H. V. Atkinson, and H. Jones, "Effect of Magnesium Alloying Additions on Infiltration Threshold Pressure and Structure of SiC Powder Compacts Infiltrated Al-Based Melts," *J. Mater. Sci.*, **32** 289-94 (1997).
18. E. Candan, H. V. Atkinson, and H. Jones, "Effect of Ceramic Particle Size and Applied Pressure on Time to Complete Infiltration of Liquid Aluminum into SiC Powder Compacts," *J. Mater. Sci.*, **35**, 4955-60 (2000).
19. J. Narcisco, A. Alonso, A. Pamies, C. Garcia-Cordavilla, and E. Louis, "Wettability of Binary and Ternary Alloys of the System Al-Si-Mg with SiC Particulates," *Scripta Metall. Mater.*, **31** [1] 1495-500 (1994).
20. T. R. Jonas, J. A. Cornie, and K. C. Russell, "Infiltration and Wetting of Alumina Particulate Performs by Aluminum and Aluminum-Magnesium Alloys," *Metall Mater.*

Trans., **26A** 1491-97 (1995).
21. A. Alonso, C. Garcia-Cordavilla, E. Louis, J. Narciso, and A. Pamies, "Evaluation of the Wettability of Al-Pb and Al-Sn Alloys with SiC and Alumina Particulates by Means of Pressure Infiltration," *J. Mater. Sci.*, **19** 4729-35 (1994).
22. J. Narciso, A. Alonso, A. Pamies, C. Garcia-Cordavilla, and E. Louis, "Factors Affecting Pressure Infiltration of Packed SiC Particulates by Liquid Aluminum," *Metall. Mater. Trans.*, **26A** 983-90 (1995).
23. J. M. Molina, R. Arpon, R. A. Saravanan, C. Garcia-Cordavilla, E. Louis, and J. Narciso, "Threshold Pressure for Infiltration and Particle Specific Surface Area of Particle Compacts with Bimodal Size Distributions," *Scripta Mater.*, **51** 623-27 (2004).
24. E. Breval, M. K. Aghajanian, J. P. Biel, and S. Antolin, "Structure of Aluminum Nitride/Aluminum and Aluminum Oxide/Aluminum Composites Produced by the Directed Oxidation of Aluminum," *J. Am. Ceram. Soc.*, **76** [7] 1865-68 (1993).
25. Y. Kajikawa, T. Nukami, and M. C. Flemings, "Pressureless Infiltration of Aluminum Metal-Matrix Composites," *Metall. Trans.*, **26A** 2155-59 (1995).
26. A. R. Kennedy, J. D. Wood, and B. M. Weager, "The Wetting and Spontaneous Infiltration of Ceramics by Molten Copper," *J. Mater. Sci.*, **35** 2909-12 (2000).
27. W. B. Johnson and B. Sonuparlak, "Diamond/Al Metal-matrix Composites Formed by the Pressureless Metal Infiltration Process," *J. Mater. Res.*, **8** [5] 1169-73 (1993).
28. J. T. Burke, C. C. Yang, and S. J. Canino, "Processing of Cast Metal-Matrix Composites," in *Cast Metal-Matrix Composites*, D.M. Stefanescu and S. Sen (eds.), Amer. Foundry Soc., Des Plaines, IL 141-51 (1994).
29. T. R. Fletcher, J. A. Cornie, and K. C. Russel, "Wettability of SiC Particulates with Zn and Zn-Al Alloys," in *Cast Reinforced Metal Composites*, Fishman and Dhingra (eds.), Amer. Soc. for Materials, Materials Park, OH 21-5, (1988).
30. N. Eustathopoulos, M. G. Nicholas, and B. Drevet, *Wettability at High Temperatures*, Pergamon (1999).
31. J. V. Naidich, "The Wettability of Solids by Liquid Metals," in *Progress in Surface and Membrane Science*, D. A. Cadenhead and J. F. Danielli (eds.), Academic Press, New York, NY 353, (1981).
32. R. Asthana and P. K. Rohatgi, "On the Melt Infiltration of Copper Coated Silicon Carbide with an Al Alloy," *Compos. Manuf.*, **3** [2] 119-23 (1992).
33. B. Palosz, in *International Workshop on Processing and Characterization of Nanomaterials,* Warsaw, Oct 8-10, 2003.
34. D. Goldberg, Y. Bando, K. Kurashima, and T. Sato, "Synthesis and Characterization of Ropes Made of BN Multiwalled Nanotubes," *Scripta Mater.*, **44** 1561 (2001).
35. N. Sobczak and R. Asthana, "The Role of Interfacial Phenomena in Wetting-Bonding Relationship in Al/Ceramic Couples," *Ceramic Transactions*, vol. 158, eds.: Weil, Reimanis, and Lewinsohn, 3-17, *Am. Ceramic Society*, Weterville, OH (2005).
36. N. Sobczak, R. Asthana, M. Ksiazek, W. Radziwill, and B. Mikulowski, "The Effect of Temperature, Alloying, and Substrate Coatings on the Relationship between Contact Angle and Interface Strength in Al_2O_3/Al Couples," *Metall. Mater. Trans.*, **35A** 911-24 (2004).
37. N. Sobczak, "Wettability and Reactivity between Molten Aluminum and Selected Oxides," in *Bulk and Graded Nanometals*, K. J. Kurzydlowski and Z. Pakiela (Eds.), Trans Tech Publications Ltd, Published in Solid State Phenomena, vols. 101-102, pp. 221-226 (2005).
38. N. Sobczak, L. Stobierski, W. Radziwill, M. Ksiazek, and M. Warmuzek, "Wettability and Interfacial Reactions in Al/TiO_2," in *Surface & Interface Analysis,* Special issue, **36** 1067-70 (2004).
39. N. Sobczak, R. Asthana, W. Radziwill, M. Ksiazek, R. Nowak, and A. Kudyba, "The Role of Aluminum Oxidation in the Wetting-Bonding Relationship of Al/Ceramic Couples," in *Proc. Int. Symp. Advanced Structural and Functional Material Design,* Osaka (Japan), 10-12 Nov., 2004.
40. N. Sobczak, K. Nogi, H. Fujii, T. Matsumoto, K. Tamada, and R. Asthana, "The Effect of Cr Thin Films on Wettability and Bonding in Ni/Alumina Couples," in *Joining of Advanced & Specialty Materials,* Indacochea *et al.* (eds.), ASM International, Materials Park, OH, 108-15 (2003).
41. V. Laurent, D. Chatain, C. Chatillon, and N. Eustathopoulos, "Wettability of Monocrystalline Alumina by Al between Its Melting Point and 1273 K," *Acta Mater.*, **36** 1797 (1988).
42. J. D. Seitz, G. R. Edwards, G. P. Martins, and P. Q. Campbell, "Infiltration Mechanisms and Kinetics of Liquid Aluminum," in *Interfaces in Metal-Ceramic Composites*, R.Y. Lin *et al.* (eds.), The Minerals, Metals & Materials Soc., 197-212 (1989).
43. R. Asthana, "Infiltration Processing of Single-Crystal SiC Platelet-Reinforced 2014 Al Composites," *Ph.D. Thesis*, University of Wisconsin-Milwaukee (1991).
44. A. Alonso, A. Pamies, J. Narcisco, C. Garcia-Cordovilla, and E. Louis, "Evaluation of the Wettability of Liquid Aluminum with Ceramic Particulates (SiC, TiC, Al_2O_3) by Means of Pressure Infiltration," *Metall. Trans.*, **24A** 1423-32 (1993).
45. J. Narcisco, C. Garcia-Cordovilla, and E. Louis, "Pressure Infiltration in a Reactive System: Packed SiC Particulates Infiltrated by Pure Silver with Dissolved Oxygen," *Acta Mater.*, **45** [12] 5111-18 (1997).
46. A. Alonso, J. Narcisco, A. Pamies, C. Garcia-Cordovilla, and E. Louis, "Effect of K_2ZrF_6 Coatings on Pressure Infiltration of Packed SiC Particulates by Liquid Aluminum," *Scripta Mater.*, **29** 1559-64 (1993).
47. J. D. Muscat and R. A. L. Drew, "Modeling the Infiltration Kinetics of Molten Aluminum into Porous Titanium Carbide," *Metall. Trans.*, **25A** 2357 (1994).
48. D. Muscat, R. L. Harris, and R. A. L. Drew, "The Effect of Pore Size on the Infiltration Kinetics of Aluminum in Titanium Carbide Preforms," *Acta Metall. Mater.*, **42** [12] 4155-63 (1994).
49. D. Muscat and R. A. L. Drew, "Infiltration Kinetics of Aluminum in Titanium Carbide Preforms," in *Proc. Int. Conf. High Temperature Capillarity*, 29 June-2 July, 1997, Krakow, Poland, eds. N. Eustathopoulos and N. Sobczak, 261-267.
50. L. J. Masur, A. Mortensen, J. A. Cornie, and M. C. Flemings, "Infiltration of Fibrous Preforms by a Pure Metal:

Part II. Experiments," *Metall. Trans.*, **20A** 2549-57 (1989).
51. P. Sangsuwan, S. N. Tewari, J. E. Gatica, M. Singh, and R. Dickerson, "Reactive Infiltration of Silicon Melt through Microporous Amorphous Carbon Preforms," *Metallurgical & Materials Transactions*, **30B** 933-44 (1999).
52. A. Mortensen and T. Wong, "Infiltration of Fibrous Performs by a Pure Metal: Part III. Capillary Phenomena," *Metall. Trans.*, **21A** 2257-63 (1990).
53. E. O. Einset, "Analysis of Reactive Melt Infiltration," *J. Amer. Ceramic Soc.*, **79** [2] 333 (1996).
54. A. Mortensen, C. San Marchi, and V. J. Michaud, "Capillarity in Infiltration Processing: A Review of Principles and their Extension to Reactive Infiltration," in *Proc. Int. Conf. High Temperature Capillarity*, 29 June-2 July, 1997, Krakow (Poland), eds. N. Eustathopoulos and N. Sobczak, 249-260.
55. C. García-Cordovilla, J. Narciso, R. Arpó, and E. Louis, *J. Mater. Sci. Lett.*, **20** [5] 405-07 (2001).
56. J. X. Zhang, R. S. Chandel, and H. P. Seow, *Science and Technology of Welding and Joining*, **7** [3] 182-86 (2002).
57. R. M. Crispin and M. G. Nicholas, "The Wetting and Bonding Behavior of Some Nickel Alloy-Alumina Systems," *J. Mater. Sci.*, **11** 17 (1976).
58. G. P. Martins, D. L. Olson, and G. R. Edwards, "Modeling of Infiltration Kinetics for Liquid Metal Processing of Composites, *Metall. Trans.*, **19B** 95-101 (1988).
59. G. L. Batten, "Liquid Imbibition in Capillaries and Packed Beds," *J. Colloid Interface Sci.*, **102** [2] 513 (1984).
60. R. E. Loehman, K. Ewsuk, W. F. Fahrenholtz, and B. B. Lakshman, "Ceramic-Metal Composite Formation by Reactive Metal Penetration," in *Key Engineering Materials*, **127-131** 431-38 (1997).
61. V. J. Michaud and A. Mortensen, "Capillarity in Isothermal Infiltration of Alumina Fiber Performs with Aluminum," *Metall. Trans.*, **25A** 2145-52 (1994).
62. V. M. Kevorkijan, "The Reactive Infiltration of Porous Ceramic Media by a Molten Aluminum Alloy," *Composites Sci. & Tech.*, **59** 683-86 (1999).
63. C. Toy and W. D. Scott, "Ceramic-Metal Composite Produced by Melt Infiltration," *J. Am. Ceram. Soc.*, **73** [1] 97 (1990).
64. V. N. Eremenko and N. D. Lesnik, "The Kinetics of the Infiltration of Porous Materials with Liquid Metals," *Role of Surface Phenomena in Metallurgy*, V. N. Eremenko (ed.), 113, Consultant Bureau, NY.
65. E. Taheri-Nassaj, M. Kobashi, and T. Choh, "Fabrication and Analysis of an in-situ TiB_2/Al Composite by Reactive Spontaneous Infiltration," *Scripta Mater.*, **34** [8] 1257-65 (1996).
66. E. Fitzer and R. Gadow, "Fiber-Reinforced Silicon Carbide," *Am. Ceram. Soc. Bull.*, **65** 326-35 (1986).
67. P. Pampuch, E. Walasek, and J. Bialoskorski, *Ceramics International*, **12** 99 (1986).
68. W. P. Minnear, "Interfacial Energies in the Si/SiC System and the Si+C Reaction," *Comm. J. Am. Ceram. Soc.*, Jan, C-10-11 (1982).
69. P. Sangsuwan, J. A. Orejas, J. E. Gatica, S. N. Tewari, and M. Singh, "Reaction-Bonded Silicon Carbide by Reactive Infiltration," *Ind. Eng. Chem. Res.*, **40** 5191-98 (2001).
70. J. G. Li and H. Hausner, "Wetting and Infiltration of Graphite Materials by Molten Silicon," *Scripta Metall. Mater.*, **32** [3] 377-82 (1995).
71. R. P. Messner and Y.-M. Chiang, "Liquid-Phase Reaction Bonding of Silicon Carbide Using Alloyed Silicon-Molybdenum Melts," *J. Am. Ceram. Soc.*, **73** [5] 1193-200 (1990).
72. E. S. Nelson and P. Colella, "Parametric Study of Reactive Melt Infiltration," *NASA TM 2000-209802*, March 2000, NASA Glenn Research Center, Cleveland, OH.
73. G. Rajesh and R. B. Bhagat, "Infiltration of Liquid Metals in Porous Compacts: Modeling of Permeabilities During Reactive Melt Infiltration," *Transport in Porous Media*, **36** [1] 43-68 (1999).
74. M. G. Nicholas and S. D. Peteves, "Reactive Joining: Chemical Effects on the Formation and Properties of Brazed and Diffusion-Bonded Interfaces," *Scripta Mater.*, **31** [8] 1091-96 (1994).
75. R. Asthana, "An Empirical Correlation between Contact Angles and Surface Tension in Some Ceramic-Metal Systems," *Metall. Trans.*, **25A** 225-30 (1994).
76. E. Fritzer and R. Gadow, "Investigations of the Reactivity of Different Carbons with Liquid Silicon," in *Proc. Int. Symp. Ceramic Components for Engines* (1983), 561-72 (1984), KTK Sci. Publ. (Tokyo).
77. R. Asthana, "Interface- and Diffusion-limited Capillary Rise of a Reactive Melt with a Transient Contact Angle," *Metall. Mater. Trans.*, **33A** 2119-28 (2002).
78. R. Asthana, "On Reactive Capillary Flow with a Dynamic Contact Angle," *J. Mater. Processing & Manufacturing Sci.*, **10** [4] 187-97 (2003).
79. R. Asthana, "Dissolutive Capillary Penetration with Expanding Pores and Transient Contact Angles," *J. Colloid Interface Sci.*, **231** 398-400 (2000).
80. R. Asthana, "Dynamic Wetting Effects During Infiltration of Metals," *Scripta Mater.*, **38** [8] 1203-10 (1998).
81. M. Singh and D. Behrendt, "Reactive Melt Infiltration of Silicon-Molybdenum Alloys into Microporous Carbon Preforms," *Mater. Sci. Eng.*, **A194** 193-200 (1995).
82. T. J. Whelan and A. T. Anderson, "Wetting of SiC, Si_3N_4, and Carbon by Si and Binary Si Alloys," *J. Am. Ceram. Soc.*, **58** [9] 396-99 (1975).
83. N. Sobczak, "Improvement of Wetting and Bonding of Dissimilar Materials," in *Interfacial Science in Ceramic Joining*, Bellosi *et al.*(eds.), Kluwer Academic Publishers, The Netherlands, 27-42 (1998).
84. D. Y. Kwok, C. J. Budziak, and A. W. Neumann, "Measurements of Static and Low Rate Dynamic Contact Angles by Means of an Automated Capillary Rise Technique," *J. Colloid Interface Sci.*, **173** 143-50 (1995).
85. P. G. De Gennes, "Wetting: Statics and Dynamics," *Rev. Mod. Phys.*, **57**, 827-63 (1985).
86. T. D. Blake and J. M. Haynes, *J. Colloid Interface Sci.*, **30** 421-23 (1969).
87. P. Joos, P. Van Remoortere, and M. Bracke, "The Kinetics of Wetting in a Capillary," *J. Colloid Interface Sci.*, **136** [1] 189-97 (1990).
88. N. Sobczak, "Wetting, Structure and Properties of Al/Al_2O_3 Interfaces," *Kompozyty*, **3** [7] 301-12 (2003).
89. N. Sobczak, J. Sobczak, and P. K. Rohatgi, in *Proc. ECO-*

MAP-98, Nov. 23-29, 1998, Kyoto, High-Temperature Society of Japan 195-205 (1999).

90. E. Saiz and A. P. Tomsia, "Kinetics of Metal-Ceramic Composite Formation by Reactive Penetration of Silicates with Molten Aluminum," *J. Am. Ceram. Soc.*, **81** [9] 2381-93 (1998).
91. R. E. Loehman, K. Ewsuk, and A. P. Tomsia, "Synthesis of Alumina-Al Composites by Reactive Metal Penetration," *J. Am. Ceram. Soc.*, **79** [1] 27-32 (1996).
92. R. E. Loehman, K. G. Ewsuk, W. F. Fahrenholtz, and B. B. Lakshman, "Ceramic-Metal Composite Formation by Reactive Metal Penetration," in *Key Eng. Mater.*, **127-131** 431-38 (1997).
93. N. Sobczak, J. Sobczak, P. Rohatgi, M. Ksiazek, W. Radziwill, and J. Morgiel, "Interaction between Ti or Cr Containing Copper Alloys and Porous Graphite Substrate," in *Proc. 2nd International Conference on High-Temperature Capillarity (HTC-2)*, 1997, N. Eustathopoulos and N. Sobczak (eds.), Foundry Research Institute, Krakow, Poland (1997), 146-51.
94. N. Grigorenko, V. Poluyanskaya, N. Eustathopoulos, and Y. Naidich, in *Interfacial Science of Cermaic Joining*, Bellosi *et al.* (eds.), Kluwer Academic Publishers, Boston, 69-78 (1998).
95. G. Levi and W. D. Kaplan, "Oxygen Induced Interfacial Phenomena During Wetting of Alumina by Liquid Aluminum," *Acta Mater.*, **50** 75-88 (2002).
96. M. Singh and D. R. Behrendt, "Reactive Melt Infiltration of Silicon-Niobium Alloys in Microporous Carbon," *J. Mater. Res.*, **7** 1701-08 (1994).
97. J. M. Fernandez, A. Munoz, A. R. de Arellano Lopez, F. M. Varela-Feria, A. Dominiguez-Rodriguez, and M. Singh, "Microstructure-Mechanical Property Correlation in Siliconized Silicon Carbide Ceramics," *Acta Materialia*, **51** 3259-75 (2003).
98. M. Singh and D. R. Behrendt, "Studies on the Reactive Melt Infiltration of Silicon and Silicon-Molybdenum Alloys in Porous Carbon," *NASA TM-105860*, NASA Lewis Research Center (1992).
99. A. Munoz, J. Martinez-Fernandez, F. M. Varela-Feria, and M. Singh, in *Joining of Advanced & Specialty Materials II*, M. Singh *et al.* (eds.), ASM International, Materials Park, 25 (2000).